THE JOURNAL OF BIOLOGICAL CHEMISTRY
Vol. 279, No. 44, Issue of October 29, pp. 46057–46064, 2004

Printed in U.S.A.

Role of βAsn-243 in the Phosphate-binding Subdomain of Catalytic Sites of *Escherichia coli* F_1-ATPase*

Received for publication, July 7, 2004, and in revised form, July 28, 2004
Published, JBC Papers in Press, August 20, 2004, DOI 10.1074/jbc.M407608200

Zulfiqar Ahmad and Alan E. Senior‡

From the Department of Biochemistry and Biophysics, University of Rochester Medical Center, Rochester, New York 14642

In the catalytic mechanism of ATP synthase, phosphate (P_i) binding and release steps are believed to be correlated to γ-subunit rotation, and P_i binding is proposed to be prerequisite for binding ADP in the face of high cellular [ATP]/[ADP] ratios. In x-ray structures, residue βAsn-243 appears centrally located in the P_i-binding subdomain of catalytic sites. Here we studied the role of βAsn-243 in *Escherichia coli* ATP synthase by mutagenesis to Ala and Asp. Mutation βN243A caused 30-fold impairment of F_1-ATPase activity; 7-chloro-4-nitrobenzo-2-oxa-1,3-diazole inhibited this activity less potently than in wild type and P_i protected from inhibition. ADP-fluoroaluminate was more inhibitory than in wild-type, but ADP-fluoroscandium was less inhibitory. βN243D F_1-ATPase activity was impaired by 1300-fold and was not inhibited by ADP-fluoroaluminate or ADP-fluoroscandium. 7-chloro-4-nitrobenzo-2-oxa-1,3-diazole activated βN243D F_1-ATPase, and P_i did not affect activation. We conclude that residue βAsn-243 is not involved in P_i binding directly but is necessary for correct organization of the transition state complex through extensive involvement in hydrogen bonding to neighboring residues. It is also probably involved in orientation of the "attacking water" and of an associated second water.

ATP synthase is the enzyme responsible for ATP synthesis by oxidative phosphorylation or photophosphorylation in membranes of bacteria, mitochondria, and chloroplasts. In its simplest form, exemplified by the *Escherichia coli* enzyme studied here, it contains eight different subunit types. Three catalytic sites, located at the interfaces of α and β subunits in the membrane-extrinsic $\alpha_3\beta_3$ hexagon, operate in concert to synthesize ATP. Reactions at the catalytic sites are controlled by rotation of the γ subunit within the $\alpha_3\beta_3$ hexagon. The γ subunit is part of the "rotor," composed of γ, ϵ, and a ring of *c* subunits. Passage of protons down the transmembrane proton gradient, through the membrane-buried interface between the c_{ring} and the *a* subunit, energizes the rotor. A "stator" immobilizes the catalytic sites during rotation. Consisting of the $b_2\delta$ subunits, the stator is attached to *a* subunit in the membrane and to the $\alpha_3\beta_3$ hexagon. Experimentally, the enzyme can be resolved readily into water-soluble F_1 and water-insoluble F_0 sectors, which correspond to the membrane-extrinsic $\alpha_3\beta_3\gamma\delta\epsilon$ and membrane-located ab_2c_{ring} subcomplexes, respectively. F_1 retains catalytic ATPase activity (a physiological activity in *E. coli*) and is used extensively for studies of the catalytic sites. Current reviews of ATP synthase structure and function may be found in Refs. 1–4. Novel experimental studies establishing proton gradient-driven subunit rotation and rotation-driven ATP synthesis are described in Refs. 5 and 6.

P_i binding and release steps are believed to be important in the catalytic mechanism of the enzyme because they are "energy-linked" and hence intimately linked to subunit rotation (reviewed in Refs. 1–3). Further, we have proposed that proton gradient-mediated P_i binding is an important factor in the ability of the enzyme to bind ADP during ATP synthesis in the face of an apparently prohibitive ATP/ADP cellular concentration ratio (1, 2). Thus studies on determinants of P_i binding in catalytic sites are likely to be valuable in understanding the catalytic mechanism. In a recent paper (7), we found that βArg-246[1] is one residue that is important for binding of P_i.

X-ray crystallography studies by Walker, Leslie, and colleagues (8–10) have revealed the structure of the P_i-binding subdomain in ATP synthase catalytic sites. Fig. 1, *A–C*, shows the structures of catalytic sites containing the transition state analog MgADP-AlF_4^- (Fig. 1*A*), the late transition state/early ground state analog MgADP-AlF_3 (Fig. 1*B*), and the posthydrolysis state with MgADP and SO_4^{2-} (Fig. 1*C*), respectively. In Fig. 1, *A* and *B*, fluoroaluminate is believed to be in the position of the γ-phosphate, and in Fig. 1*C*, SO_4^{2-} is thought to mimic P_i. The central location of residue βAsn-243 in the P_i-binding subdomain is evident from Fig. 1. The ND2 atom of the Asn side chain points toward the γ-P/P_i moiety, whereas the OD1 atom points toward neighboring residues that line the end of the P_i-binding pocket. Also, it may be noted that βAsn-243 lies close to βArg-246, the P_i-binding residue mentioned above. For these reasons, we decided to investigate the possible role of βAsn-243 in P_i binding.

Direct measurement of P_i binding to F_1 or intact ATP synthase catalytic sites is difficult due to low affinity for P_i in absence of a proton gradient (1, 2). The x-ray crystallography studies suggested alternative, indirect approaches, namely the use of surrogates for P_i or the γ-P of ATP such as fluoroaluminate, fluoroscandium, and fluoroberyllate, or the use of NBD-Cl,[2] which reacts specifically with residue βTyr-297 (10), located at the end of the P_i binding subdomain (Fig. 1*D*). The value of this last approach is enhanced by the fact that protection from covalent reaction with NBD-Cl is afforded by P_i in the concentration range 2–10 mM, as was first shown by Perez *et al.* (11) with mitochondrial membranes and confirmed by us (7) in *E. coli* F_1 and membrane F_1F_0. Here we utilized these methods to study the role of residue βAsn-243 in the P_i-binding subdo-

* This work was supported by National Institutes of Health Grant GM25349 (to A. E. S.). The costs of publication of this article were defrayed in part by the payment of page charges. This article must therefore be hereby marked "*advertisement*" in accordance with 18 U.S.C. Section 1734 solely to indicate this fact.

‡ To whom correspondence should be addressed: Dept. of Biochemistry and Biophysics, Box 712, University of Rochester Medical Center, Rochester, NY 14642. Tel.: 585-275-6645; Fax: 585-271-2683; E-mail: alan_senior@urmc.rochester.edu.

[1] *E. coli* residue numbering used throughout.

[2] The abbreviations used are: NBD-Cl, 7-chloro-4-nitrobenzo-2-oxa-1,3-diazole; DTT, dithiothreitol.

main. It was anticipated that this residue might not be directly involved in P_i binding, since it lacks positive charge; rather, it appeared more likely from its central position in the P_i-binding subdomain to be involved in hydrogen bond formation with surrounding residues, including βArg-246, and also with water molecules, including, indirectly, the putative "attacking water." We mutagenized residue βAsn-243 to Ala to remove the side chain and eliminate hydrogen bond interactions and to Asp to introduce a negative charge and retain hydrogen bonding capacity. The two mutant enzymes, while both functionally impaired, showed different properties when subjected to assays aimed at examination of P_i binding and transition state characteristics, allowing deductions about the role of the natural residue βAsn-243.

EXPERIMENTAL PROCEDURES

Purification of E. coli F_1, Assay of ATPase Activity of Purified F_1, and Measurement of Growth Yield in Limiting Glucose Medium—F_1 was purified as described in Ref. 12. Prior to experiments, F_1 samples (100 μl) were passed twice through 1-ml centrifuge columns (Sephadex G-50) equilibrated in 50 mM $TrisSO_4$, pH 8.0, to remove catalytic site-bound nucleotide (13). ATPase activity was measured in 1 ml of assay buffer containing 10 mM NaATP, 4 mM $MgCl_2$, 50 mM $TrisSO_4$, pH 8.5. Specific activity was measured at 30 °C (wild type, βN243A) or 37 °C (wild type, βN243D). Measurements of inhibition of ATPase activity by inhibitors were done at 23 °C (wild type, βN243A) or at 37 °C (βN243D). Reactions were started by the addition of enzyme and stopped by the addition of SDS to 3.3% final concentration. P_i released was assayed as described in Ref. 14. For wild-type F_1, reaction times were 2–10 min. For mutant enzymes, reaction times were 30 min (βN243A) or 120 min (βN243D). All reactions were shown to be linear with time and protein concentration. Growth yield in limiting glucose was measured as described in Ref. 15.

E. coli Strains—For purified F_1, wild-type strain SWM1 was used (16). For fluorescence titrations with purified F_1, strain SWM4 (βY331W) (17) was used as the "wild-type." Mutant strains were βN243A/βY331W and βN243D/βY331W, both in strain DK8 (18) and constructed as below.

Construction of Mutant Strains of E. coli—pSN6 is a plasmid containing the βY331W mutation from plasmid pSWM4 (17) introduced on a SacI-EagI fragment into pBWU13.4 (19), which expresses all of the ATP synthase genes. The template for oligonucleotide-directed mutagenesis was M13mp18 containing the HindIII-XbaI fragment from pSN6. Mutagenesis was by the method of Vandeyar *et al.* (20). Mutagenic oligonucleotides were as follows: βN243A (CTGCTGTTCGTCGACGCCATCTATCGTTAC, where the underlined bases introduce the mutation and a new SalI site) and βN243D (CTGTTCGTTGACGATATCTATCGTTAC, where the underlined bases introduce the mutation and a new EcoRV site). DNA sequencing was performed to confirm the presence of mutations and absence of undesired changes in sequence, and the mutations were transferred to pSN6 on SacI-EagI fragments, generating the new plasmids pZA3 (βN243A/βY331W) and pZA4 (βN243D/βY331W), respectively. Each plasmid was transformed into strain DK8 (18) containing a deletion of ATP synthase genes for expression of the mutant enzymes.

Protein Concentration, Purity, Subunit Composition, and Trp Content of Mutant Enzymes—Protein concentration was determined by the Bradford method (21). Purity and subunit composition was determined by SDS-gel electrophoresis (22). Trp content was determined by incubation of varied amounts of enzyme at room temperature for 15 min in 6.3 M guanidine hydrochloride, and then fluorescence emission at 360 nm (λ_{exc} = 295 nm) was measured and compared with wild-type enzyme and *N*-acetyl-tryptophanamide as references. For calculations, 1 mg/ml F_1 was taken as 2.62 μM.

Fluorescence Titrations—The method utilizes the quench of fluorescence of introduced residue βTrp-331 that occurs upon nucleotide binding to catalytic sites (23). Titration with MgADP and MgATP was carried out in 50 mM $TrisSO_4$, pH 8.0, 2.5 mM $MgSO_4$ at room temperature. NaADP and NaATP were added incrementally. For ATP and ADP titrations, the buffer was 50 mM $TrisSO_4$, pH 8.0, 0.5 mM EDTA. Excitation was at 295 nm, emission was at 360 nm in a SPEX Fluorolog 2 spectrofluorometer. Final enzyme concentration in the cuvette was 150–200 nM, and enzyme was incubated 10 min at room temperature before titration was begun. Background signals due to buffer were subtracted, and volume and inner filter effects were corrected by carrying out parallel titrations with wild-type F_1. Calculation of nucleotide binding parameters was accomplished by fitting theoretical curves to the measured data points using SigmaPlot. The binding models used are described in Table II and in Refs. 23 and 24.

TABLE I
Effects of βAsn-243 mutations on cell growth and F_1-ATPase activity

Mutation[a]	Growth on succinate	Growth yield in limiting glucose[b]	ATPase activity of purified F_1[b]
		%	μmol/min/mg
Wild type	+++	100	28[c]; 42[d]
Null	−	46	−
βN243A	+	88	0.95[c]
βN243D	−	51	0.033[d]

[a] Wild type, pBWU13.4/DK8; null, pUC118/DK8.
[b] Data are means of six determinations that agreed closely (±10%).
[c] Measured at 30 °C.
[d] Measured at 37 °C.

Inhibition of ATPase Activity—For fluoroaluminate, fluoroscandium, and fluoroberyllate inhibition, F_1 was incubated for 60 min at 23 °C in 50 mM $TrisSO_4$, 2.5 mM $MgSO_4$, 1 mM NaADP, and 12 mM NaF at a protein concentration of 0.4–2.0 mg/ml in the presence of $AlCl_3$, $ScCl_3$, or $BeSO_4$, added at varied concentrations (see "Results"). 50-μl aliquots were then added to 1 ml of ATPase assay buffer, and activity measured as above. It was confirmed in control experiments that no inhibition was seen if $MgSO_4$, NaADP, or NaF was omitted. For NBD-Cl inhibition of purified F_1, NBD-Cl was prepared as a stock solution in dimethyl sulfoxide and protected from light. Enzyme (0.4–2.0 mg/ml) was reacted with NBD-Cl for 60 min in the dark, at 23 °C, in 50 mM $TrisSO_4$, pH 8.0, 2.5 mM $MgSO_4$, and then 50-μl aliquots were transferred to 1 ml of ATPase assay buffer to determine activity. Where protection from NBD-Cl inhibition by ADP or P_i was determined, F_1 was preincubated 60 min with protecting agent before the addition of NBD-Cl. $MgSO_4$ was present, equimolar with ADP or P_i. Control samples containing the ligand without added NBD-Cl were included. Neither P_i (up to 50 mM) nor MgADP (up to 10 mM) had any inhibitory effect alone. For measurement of azide inhibition, sodium azide at varied concentrations was added directly to the ATPase assay buffer, to which F_1 was added to start the reaction.

RESULTS

Properties of βN243A and βN243D Mutants of E. coli ATP Synthase—The role of residue βAsn-243 in the phosphate-binding subdomain of *E. coli* ATP synthase catalytic sites was investigated by mutagenesis. Mutants βN243A and βN243D were obtained by oligonucleotide-directed mutagenesis and expressed in the ATP synthase complex in strain DK8, which lacks all ATP synthase structural genes. The additional mutation βY331W was present in both cases to allow monitoring of nucleotide binding affinity and stoichiometry in purified F_1 by fluorescence titration. It has been previously established that the βY331W mutation alone does not significantly impair ATP synthase function (17). Table I shows that the mutation βN243A reduced growth yield moderately and allowed partial growth on plates containing succinate, demonstrating that it partly impaired oxidative phosphorylation *in vivo*.[3] The βN243D mutation prevented growth on succinate plates and reduced growth yield strongly, showing that oxidative phosphorylation was greatly impaired.

Purified F_1 proteins were obtained and shown to have the same subunit composition and purity as wild-type enzyme by SDS-gel electrophoresis. Trp content was 12 mol/mol in both mutant enzymes, confirming their purity. Specific ATPase activities are shown in Table I. βN243A enzyme was 30-fold less active than wild-type. Preliminary assays showed that βN243D had very low activity at the standard assay temperature of 30 °C; hence, it was necessary to assay at 37 °C for long times. We confirmed that the reaction stayed linear for at least 2 h,

[3] It should be noted that high expression in the system used increases the amount of ATP synthase in the membranes.

TABLE II
Nucleotide binding parameters of mutant enzymes

K_d values are given in μM and are means of calculated values from three or four independent titrations, which agreed closely.

	βY331W	βN243A	βN243D
ADP			
K_{d1}, K_{d2}, K_{d3}[a]	89	59	22
ATP			
K_{d1}, K_{d2}, K_{d3}[a]	76	230	289
MgADP[b]			
K_{d1}	0.06	0.07	0.02
K_{d2}	2.4	28	2.7
K_{d3}	41	151	19
MgATP[c]			
K_{d1}	0.04	0.06	1.5
K_{d2}	1.6	25	3.1
K_{d3}	35	25	78

[a] In previous work (13, 23–25), we found that titrations of βY331W F_1 with ADP or ATP were fit best by a model assuming one type of binding site. Similarly, the titrations for βN243A and βN243D were fit best by the same model.

[b] In previous work (13, 23–25, 27–29), we found that titrations of βY331W F_1 with MgADP could be fit equally well to a model with two types of binding site or to one with three types of site, but fit poorly to a model with just one type of site. Since x-ray structures (4, 8, 9) indicate that the three catalytic sites are structurally different, we used a three-site model here.

[c] Previous work (13, 23–25, 27–29) has established that titrations of βY331W F_1 with MgATP are fit best by a model with three types of binding site. The same was found here with the βN243A and βN243D mutants.

and the very low rate of nonenzymatic ATP cleavage was controlled for. βN243D F_1 ATPase activity was reduced by 1300-fold relative to wild type; thus, the introduction of Asp in place of Asn had a severe effect.

Catalytic Site Nucleotide Binding Properties of the Mutant βN243A and βN243D F_1 Enzymes—Nucleotide binding to catalytic sites of soluble F_1 was determined using the quench of fluorescence of the introduced βTrp-331. Calculated K_d values for ATP, ADP, MgATP, and MgADP are shown in Table II. In βY331W enzyme (representative of wild type) ATP and ADP are known from previous work to bind with the same affinity at all three sites (13, 24), and this behavior was also seen in the mutants. In βN243A, $K_{d(ADP)}$ was slightly lower than in βY331W, but βN243D bound ADP 4-fold more tightly than βY331W, showing that the introduced carboxyl did not appear to interact with the negative charge on ADP. In both mutants ATP binding was weakened (by 3–4-fold), with βN243D showing the larger effect. In βY331W enzyme, MgADP and MgATP bind to the three catalytic sites with widely different affinities (13, 24). This "asymmetric" behavior was retained in the mutants. The βN243A mutant bound MgADP more weakly than βY331W at site 2 (by 12-fold) and site 3 (by 4-fold), with $K_{d(ADP)}$ at site 1 similar to normal. The βN243D mutant bound MgADP more tightly than βY331W at site 1 (by 3-fold) and site 3 (by 2-fold) with $K_{d(ADP)}$ at site 2 similar to normal. βN243A bound MgATP similarly to βY331W at site 1, but with 16-fold lessened affinity at site 2 and similar affinity to βY331W at site 3, whereas βN243D bound MgATP 4-fold more weakly at site 1 and 2-fold more weakly at sites 2 and 3. Overall, except for the two cases noted where the changes in K_d were on the order of 10-fold, the changes seen were small (*e.g.* compare with previous data showing 30–4000-fold changes in other impaired mutant enzymes) (24, 25). In both mutants, all three catalytic sites would be occupied by MgADP or MgATP at saturation (~1 mM), and no general trends were evident in perturbation of nucleotide binding that could readily explain the effects seen on ATPase activity.

Inhibition of ATPase Activity of F_1 by Analogs Fluoroaluminate, Fluoroscandium, and Fluoroberyllate—Wild-type or βY331W *E. coli* F_1-ATPase is strongly inhibited by $AlCl_3$ in combination with NaF, ADP, and Mg^{2+} (26, 27). Experiments from our laboratory showed that MgADP-fluoroaluminate forms a tenaciously bound inhibitory complex with F_1 that mimics a transition state (27–29). X-ray crystallography subsequently deduced the structure of mitochondrial F_1 with both ADP-AlF_4^- and ADP-AlF_3 species bound (8, 9) (Fig. 1, *A* and *B*), from which it is clear that the fluoroaluminate moiety occupies the position of the γ-P of ATP or of P_i in the catalytic sites. Fig. 2*A* shows that the βN243A mutant F_1 was inhibited more potently than wild type by ADP-fluoroaluminate. IC_{50} values were as follows: wild type, 70 μM; βN243A, 18 μM. In contrast, the βN243D mutant was fully resistant to inhibition.

The MgADP-fluoroberyllate complex is thought to provide a tenaciously trapped ground state analog of MgATP (*e.g.* see Ref. 30). As Fig. 2*B* shows, this complex strongly inhibited the wild-type enzyme, whereas βN243A was inhibited less potently, and βN243D was resistant to inhibition. The MgADP-fluoroscandium complex has been shown to be a transition state analog in F_1-ATPase (31). It strongly inhibits wild-type enzyme (Fig. 2*C*), whereas βN243A enzyme was only partly inhibited, by ~25%, and, unexpectedly, there was stimulation in the βN243D enzyme.

In summary, the two mutant enzymes behaved divergently. The βN243D mutation uniformly disrupted interactions in the catalytic site between the enzyme and transition state or ground state analogs. The βN243A mutation had more variable consequences, in one case strengthening interaction (fluoroaluminate) and in the other two cases weakening it. The results show clearly the importance of residue βAsn-243 for correct transition state formation.

Inhibition of ATPase Activity of F_1 by Azide—Azide is a potent inhibitor of F_1-ATPases in general, although its mode of inhibition remains controversial (32, 33). It has not yet been located in x-ray structures of F_1. In one view (33), azide forms a tightly bound MgADP-N_3^- complex at catalytic sites, possibly mimicking MgADP-Pi; in another view (32), azide disrupts positive catalytic site cooperativity. Fig. 3 shows that the mutant βN243A was inhibited by 25%, whereas βN243D was inhibited by only 6% at 0.5 mM azide. It should be noted that βY331W F_1 is strongly inhibited by azide (32).

Effect of NBD-Cl on the Mutant Enzymes—NBD-Cl is a well established, potent inhibitor of F_1 ATPase activity. It reacts specifically and covalently with residue βTyr-297, which is situated at the end of the phosphate binding pocket. Fig. 1*D* shows the x-ray structure of the βE catalytic site containing the NBD-*O*-tyrosyl adduct after reaction. P_i protects against NBD-Cl inhibition (11), and this property may be used as an assay of binding of P_i in the βE catalytic site (7). Residue βAsn-243 is located very close (~3 Å) to residue β-Tyr-297 (Fig. 1, *A–C*); therefore, we were interested in studying the effects of NBD-Cl on the ATPase activities of the mutant enzymes. Fig. 4*A* shows that in contrast to wild type, which is virtually completely inhibited by NBD-Cl, βN243A F_1 was inhibited maximally by 85%. If, at the end of a 60-min incubation with 150 μM NBD-Cl, we added a further 200 μM concentration of NBD-Cl and incubated for a further 60 min, no additional inhibition occurred, showing that the fully reacted enzyme retained significant residual activity. Surprisingly, βN243D mutant F_1 showed activation of ATPase activity upon reaction with NBD-Cl (Fig. 4*B*). The addition of 4 mM DTT to the mutant enzymes after reaction with NBD-Cl reversed the effects (Fig. 5). The βN243A enzyme became reactivated, and the βN243D enzyme activity decreased. This

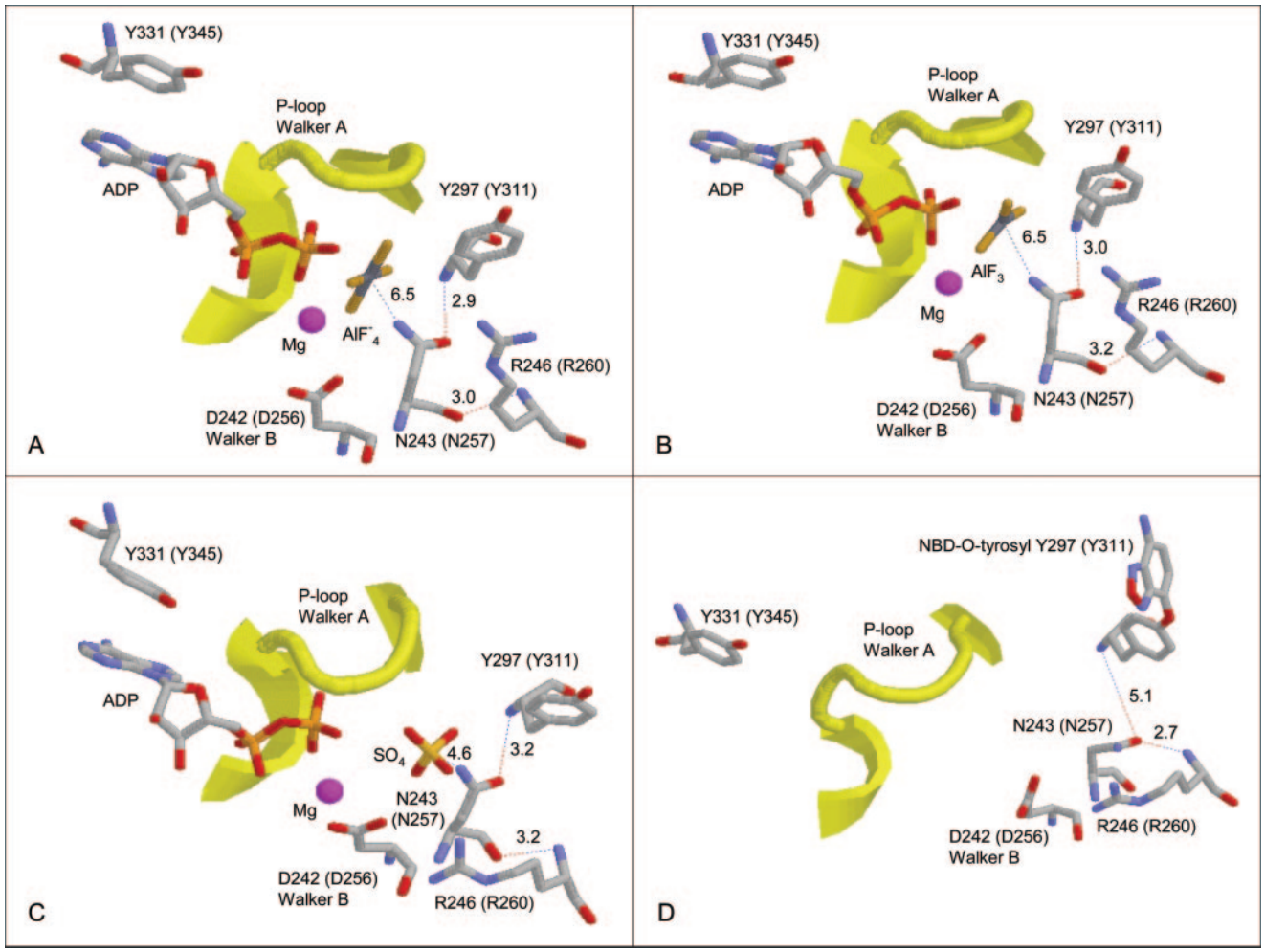

FIG. 1. **X-ray structures of catalytic sites in mitochondrial F_1-ATPase showing the phosphate binding subdomain.** *A*, the βDP site of the AlF_4^--inhibited enzyme (8). Residue numbers correspond to *E. coli* numbering with mitochondrial numbering in *parentheses*. Distances are given in Ångstroms. *B*, the βDP site in the AlF_3-inhibited enzyme (9). *C*, the βADP + P_i ("β-half-closed") site in the AlF_4^--inhibited enzyme (8). The sulfate ion is thought to occupy the position of natural P_i. *D*, reacted NBD-*O*-Tyr-297 in the βE site (10). In *A–C*, the ND2 atom of residue βAsn-243 points toward the fluoroaluminate or sulfate, with the OD1 atom pointing away. In *D*, a rotation of the Asn side chain has occurred.

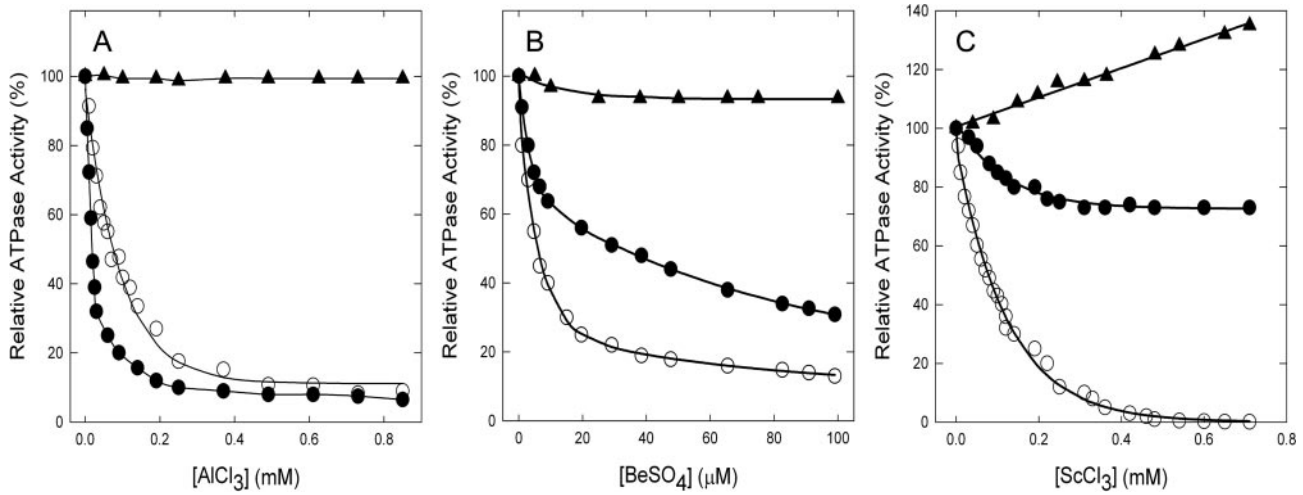

FIG. 2. **Inhibition of βN243A and βN243D mutant F_1 ATPase activity by fluoroaluminate, fluoroberyllate, and fluoroscandium.** *A*, inhibition of ATPase after preincubation for 60 min with 1 mM MgADP, 12 mM NaF, and varied $AlCl_3$. *B*, inhibition of ATPase after preincubation for 60 min with 1 mM MgADP, 12 mM NaF, and varied $BeSO_4$. *C*, inhibition of ATPase after preincubation for 60 min with 1 mM MgADP, 12 mM NaF, and varied $ScCl_3$. ○, wild-type; ●, βN243A; ▲, βN243D. Note that in this and in subsequent figures, ATPase activity was measured at 23 °C (wild type, βN243A) or 37 °C (βN243D). Data are means of at least quadruplicate experiments. Variation was ±10% between different experiments.

experiment showed that in both cases, the reaction of NBD-Cl was specifically with residue βTyr-297 (34, 35). It also assured us that the rather low ATPase activity of the βN243D mutant F_1 preparation is in fact referable to the mutant F_1 and not to a contaminant protein.

It was apparent therefore that mutation of βAsn-243 to Ala

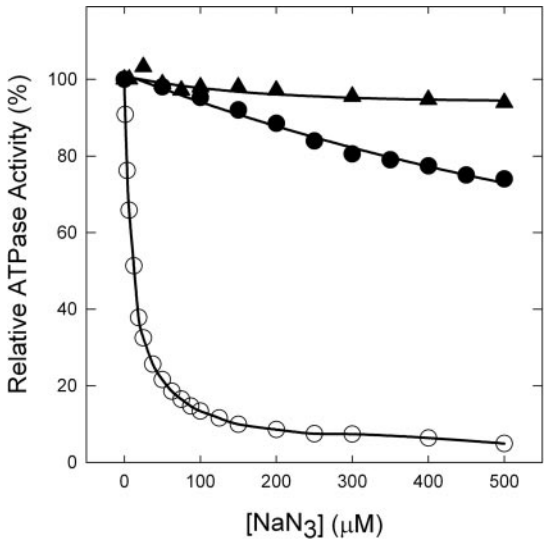

FIG. 3. **Effect of azide on βN243A and βN243D mutant F_1 ATPase activity.** Varied concentrations of sodium azide were added directly to the ATPase assay medium. ○, wild-type; ●, βN243A; ▲, βN243D. Data are means of at least quadruplicate experiments. Variation was ±10% between different experiments.

or Asp affected reactivity of the proximal βTyr-297 with NBD-Cl and produced different effects in regard to the residual ATPase activity of the fully reacted enzymes in the two mutants.

It was of interest to find out whether the ATPase activity in the NBD-Cl-reacted βN243D enzyme had become sensitive to the inhibitors MgADP-fluoroaluminate, MgADP-fluoroberyllate, or MgADP-fluoroscandium. βN243D enzyme that had been activated by preincubation with 300 μM NBD-Cl (as in Figs. 4*B* and 5) was then further incubated with MgADP, NaF, and 0.5 mM $AlCl_3$, 0.1 mM $BeSO_4$, or 0.5 mM $ScCl_3$ as in Fig. 2. In no case was inhibition seen (data not shown).

MgADP Protects against the Effects of NBD-Cl—MgADP, at relatively high concentrations required to keep the βE catalytic site occupied in time average, protects against NBD-Cl inhibition of wild-type *E. coli* F_1 and F_1F_0 (7). Fig. 6*A* shows that MgADP protected βN243A F_1 from inhibition by NBD-Cl, with 50% protection achieved at around 4 mM MgADP, similar to wild type. Incubation of either wild-type or βN243A enzyme with MgADP alone did not result in inhibition of ATPase activity, up to around 10 mM MgADP, when inhibition began to occur presumably as a result of MgADP carryover into the assay. Fig. 6*B* shows that MgADP also protected against the activation of ATPase in βN243D mutant F_1, with a similar EC_{50} of around 4 mM. These experiments showed that NBD-Cl is reacting in the βE sites in the mutants and confirmed that the low ATPase activity in βN243D is indeed referable to mutant F_1 as opposed to a contaminant, because it showed the same EC_{50} for protection by MgADP as in wild-type.

Reaction of Mutant Enzymes with NBD-Cl in the Presence of P_i—The rate of inhibition or activation of ATPase activity in βN243A and βN243D mutant F_1 by NBD-Cl was measured in the presence and absence of P_i. In wild type (Fig. 7*A*), 2.5 and 10 mM P_i had clear effects, protecting from inhibition by NBD-Cl. Similar effects were seen in βN243A (Fig. 7*B*), where reaction with NBD-Cl was slower (as was also seen in Fig. 4*A*) but nevertheless significant protection by P_i was evident. In contrast, activation of ATPase in βN243D was unaffected by the presence of P_i up to 10 mM (Fig. 7*C*).

DISCUSSION

The important role of P_i binding and release steps in the catalytic mechanism of ATP synthase has been discussed in current reviews (1, 2, 36). Early work indicating that these were "energy-linked" steps can now be interpreted as showing a direct linkage between γ-subunit rotation and events in the catalytic sites. Additionally, we have hypothesized that initial binding of P_i is a critical component of ATP synthesis mechanism because it enables selective binding of ADP in the face of a high cellular ATP/ADP concentration ratio. Progress has been delayed, however, by the inability to directly measure and distinguish P_i binding to one or another of the three catalytic sites in soluble F_1, the most amenable experimental system. This difficulty was overcome here by use of indirect methods, namely the use of fluoroaluminate, fluoroscandium, and fluoroberyllate as surrogates for P_i and/or the γ-phosphate of ATP, and an assay in which protection from NBD-Cl inhibition of ATPase activity is afforded by P_i, as reported earlier by Perez *et al.* using mitochondrial F_1 (11). X-ray structures show that residue βAsn-243 is centrally located in the P_i-binding subdomain of catalytic sites (8–10) (Fig. 1, *A–C*) with its side chain ND2 atom pointing toward the P_i/γ-P moiety and the OD1 atom pointing toward residues that demarcate the end of the P_i-binding pocket. A BLAST search showed that βAsn-243 is totally conserved. It seemed likely therefore that βAsn-243 could be involved in P_i binding, and here we used the approaches noted above to study the role of residue βAsn-243.

Mutations βN243A and βN243D were generated to remove the Asn side chain (Ala) and to substitute it by an isosteric but negatively charged side chain (Asp), respectively. This produced enzymes with distinctly different properties. βN243A impaired cellular oxidative phosphorylation somewhat and reduced purified F_1-ATPase activity by 30-fold; βN243D strongly impaired oxidative phosphorylation and reduced F_1-ATPase by 1300-fold. It was evident, therefore, that βAsn-243 does have an important role. Fluorescence titrations using the βY331W reporter probe were carried out in order to determine K_d values for ADP, ATP, MgADP, and MgATP at catalytic sites of the mutant enzymes. It was seen that all four nucleotides bound to all three catalytic sites in both mutant enzymes at saturation (~1 mM); thus, impaired ATP synthase or ATPase activity could not be ascribed to failure to fill the catalytic sites. As described under "Results," changes in K_d values were mostly small, and there was no obvious trend or trends that could be correlated with loss of function. We concluded that the functional defects in the mutant enzymes are therefore more likely to be related to reaction chemistry and/or P_i binding characteristics.

The βN243A enzyme showed different behavior toward the transition state analogs MgADP-fluoroaluminate and MgADP-fluoroscandium (Fig. 2). MgADP-fluoroaluminate was more inhibitory than in wild type, and MgADP-fluoroscandium was less inhibitory. MgADP-fluoroberyllate was also less inhibitory in βN243A than in wild type. We conclude that whereas βAsn-243 does not directly interact with the transition state nucleotide, removal of the Asn side chain changes the orientation of ligands that make contact with the transition state. A similar conclusion could apply to the MgADP-fluoroberyllate ground state analog.[4] In the βN243D enzyme, inhibition by MgADP-fluoroaluminate and MgADP-fluoroscandium was lost, showing that introduction of Asp disrupted transition state stabilization drastically. In this enzyme, MgADP-fluoroscandium even increased ATPase activity somewhat (Fig. 2*C*), an effect that we have not seen in any other enzyme and have no ready explanation for. Inhibition by MgADP-fluoroberyllate was also lost in the βN243D mutant.

[4] An X-ray structure of F_1 in complexation with MgADP-fluoroberyllate has not yet been published.

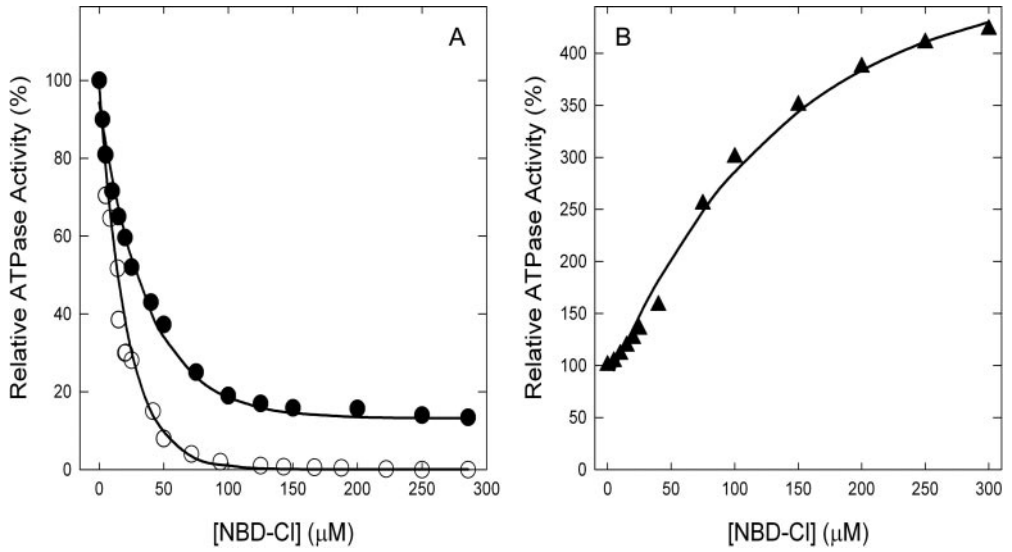

FIG. 4. **Effect of NBD-Cl on βN243A and βN243D mutant F_1 ATPase activity.** Purified F_1 was preincubated 60 min at 23 °C with varied concentrations of NBD-Cl and then assayed for ATPase activity. For details, see "Experimental Procedures." ○, wild type; ●, βN243A; ▲, βN243D. Data are means of at least quadruplicate experiments. Variation was ±10% between different experiments.

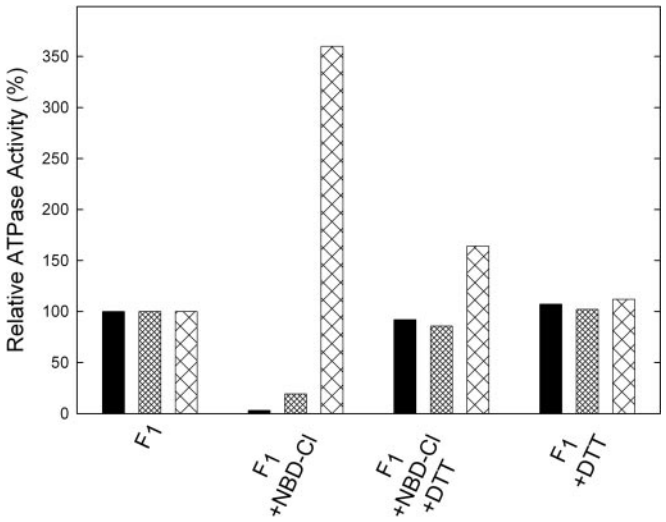

FIG. 5. **Reversal of NBD-Cl effects by DTT.** Purified F_1 was preincubated 60 min at 23 °C with or without 150 μM NBD-Cl, and then incubation was continued for a further 60 min with or without the addition of 4 mM DTT, after which ATPase was assayed. In each group of histograms the order is, from *left* to *right*, wild-type, βN243A, and βN243D. Data are means of at least triplicate experiments. Variation was ±5% between different experiments.

The mutant enzymes largely (βN243A) or almost completely (βN243D) abrogated inhibition by sodium azide. As discussed earlier, there are currently two schools of thought regarding the explanation for azide inhibition in F_1, one suggesting that azide forms a tight binding MgADP-N_3^- complex at catalytic sites that possibly mimics MgADP-P_i and the other suggesting that, at least in *E. coli* F_1, azide interrupts positive catalytic cooperativity. As is discussed below, P_i binding seems to be retained in βN243A F_1. We feel therefore that a likely explanation of the current data is that azide inhibits by interrupting catalytic cooperativity in wild-type *E. coli* F_1 and that such cooperativity is already reduced in the two mutant enzymes.

NBD-Cl inhibited ATPase activity of βN243A mutant enzyme somewhat less potently than in wild type and left a residual activity of around 15% after complete reaction. P_i at 2.5 and 10 mM concentration gave clear protection from inhibition by NBD-Cl. This result demonstrates that removal of the βAsn-243 side chain by mutagenesis to Ala did not result in loss of P_i binding in the βE catalytic site, where NBD-Cl reacts. The loss of function in βN243A must therefore be related to changes in transition state complex interactions as noted above. NBD-Cl activated the ATPase of F_1 from βN243D. The activation was DTT-reversible and MgADP-protectable, so it appeared to result from reaction of NBD-Cl with βTyr-297 in the βE site, just as the more usual inhibition of ATPase in wild-type enzyme does. The activation was not affected by presence of P_i; therefore, binding of P_i in the βE site was lost in the βN243D mutant. This, together with the severely impaired interaction with the transition state complex noted above, appears to bring about the very strong impairment of function seen in βN243D.

Fig. 1, *A–D*, shows the spatial relationship of βAsn-243 to selected residues in four x-ray crystallography structures, namely the βDP site of the AlF_4^- structure (8), the βDP site of the AlF_3 structure (9), the βADP + P_i site of the AlF_4^- structure (8), and the βE site of the NBD-Cl-reacted structure (10). We made a compilation of distances between atoms of βAsn-243 and neighboring residue atoms in these four structures (data not shown) from which it was apparent that residue βAsn-243 is in position to make hydrogen bonds with several residues within and lining the P_i binding pocket, notably with βVal-179, βIle-244, βTyr-245, βArg-246, βAla-295, and βTyr-297. In general, the interactions between βAsn-243 and other residues were the same in *A–C* of Fig. 1, but after reaction with NBD-Cl (Fig. 1*D*) several of the distances between βAsn-243 atoms and other residue atoms were significantly changed.

Using the "Deep View Swiss-Pdb Viewer" program,[5] we attempted to discern what effects the mutations might have on these distances. The results are obviously not based on real structures but lead to interesting speculations. The βN243A mutation removes all possible hydrogen bonds involving ND2 and OD1 atoms, which contribute most to interactions with neighboring residues in wild type. Loss of structural organization caused by disruption of hydrogen bonds within the P_i binding subdomain of the catalytic site is therefore a likely outcome of the βN243A mutation. This was associated with moderate loss of function, perturbation of transition state or-

[5] N. Guex, A. Diemand, M. C. Peitsch, and T. Schwede (2004) Deep View Swiss-Pdb Viewer, Version 3.7, available on the World Wide Web at us.expasy.org/spdbv/mainpage.html.

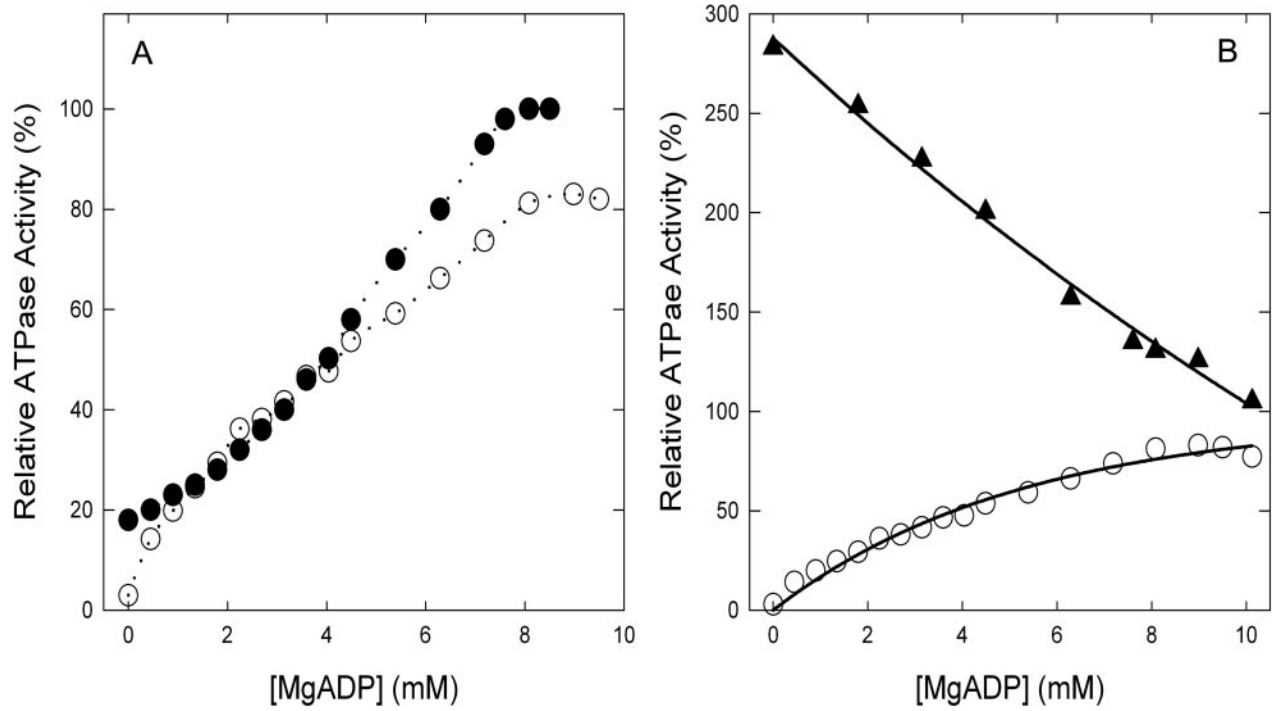

FIG. 6. **MgADP protects βN243A and βN243D mutant enzymes from inactivation/activation by NBD-Cl.** Purified F_1 was preincubated with MgADP at varied concentration for 60 min at 23 °C, and then NBD-Cl (125 μM) was added, and incubation continued for 60 min, at the end of which ATPase activity was assayed. For further details, see "Experimental Procedures." ○, wild type; ●, βN243A; ▲, βN243D. Data are means of at least quadruplicate experiments. Variation was ±10% between different experiments.

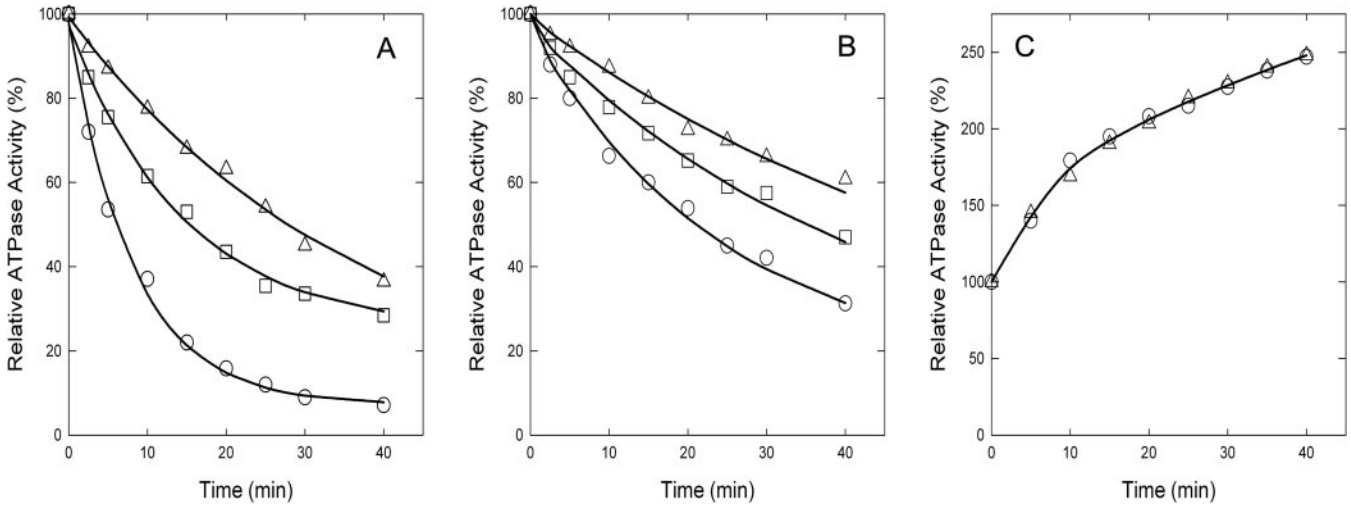

FIG. 7. **Does P_i protect against inactivation/activation by NBD-Cl in the mutant enzymes?** Purified F_1 was preincubated with P_i at 2.5 mM or 10 mM concentration for 60 min at 23 °C, and then NBD-Cl (100 μM) was added, and aliquots were withdrawn for ATPase assay at the times shown. For further details, see "Experimental Procedures." *A*, wild type. *B*, βN243A. *C*, βN243D. ○, no P_i added; □, 2.5 mM P_i; △, 10 mM P_i. Data are means of at least quadruplicate experiments. Variation was ±10% between different experiments.

ganization, and some changes in nucleotide binding characteristics, but did not lead to loss of P_i binding. In the βN243D mutation, the new atom OD2 (replacing ND2) could potentially hydrogen-bond to βVal-296, replacing the interaction with βAla-295 in wild type. Most of the other interactions listed above for βAsn-243 should be retained, since they involve the OD1 atom. There is the additional, strong possibility that charge neutralization occurs between βAsp-243 and βArg-246, given the proximity of the two residues. Thus, the more drastic effects on function seen in the βN243D mutation can be interpreted as due to formation of a different pattern of hydrogen bonds around residue β243, with charge neutralization of residue βArg-246 probably contributing strongly to loss of P_i binding. In the βN243D mutant, reaction with NBD-Cl produced apparent changes to potential hydrogen-bonding interactions, which differed from those seen in wild-type (βAsn-243) after reaction with NBD-Cl. However, exactly how they contribute to activation of ATPase in βN243D F_1 remains obscure.

The role of βAsn-243 in orienting water molecules in the catalytic site should also be discussed. X-ray structures (8, 9) have located one particular water molecule called the "attacking water" close to residue βGlu-181, the "catalytic carboxylate" residue, which is known to form part of the transition state complex (8, 9, 27). In the (βDP)AlF_4^- catalytic site, representing the transition state complex, the attacking water lies 3.3 Å from a second water, which in turn lies 2.9 Å from βAsn-243 atom ND2. The two waters lie 2.5 and 3.2 Å, respectively, from the catalytic carboxylate βGlu-181. In the (βDP)AlF_3 catalytic

site, representing a late transition state/early ground state, the attacking water is 2.8 Å from the second water, which in turn is 3.3 Å from βAsn-243 atom ND2. Mutations βN243A and βN243D could therefore be affecting the transition state structure through effects on positioning of the attacking water molecule.

In summary, residue βAsn-243 lies in the center of the P_i-binding subdomain of ATP synthase catalytic sites. It is not directly involved in P_i binding but is necessary for reaction chemistry via correct organization of the transition state complex. It is involved in extensive hydrogen bonding to neighboring residues. It is also most probably involved in orientation of the attacking water and of an associated second water. Mutation to Ala partly disrupts the transition state and has moderate inhibitory effects on function. Mutation to Asp grossly disrupts the transition state, prevents P_i binding (probably through charge neutralization of βArg-246), and results in marked dysfunction.

Acknowledgment—We thank Erich Huang for outstanding technical assistance.

REFERENCES

1. Weber, J., and Senior, A. E. (2003) *FEBS Lett.* **545,** 61–70
2. Senior, A. E., Nadanaciva, S., and Weber, J. (2002) *Biochim. Biophys. Acta* **1553,** 188–211
3. Noji, H., and Yoshida, M. (2001) J. *Biol. Chem.* **276,** 1665–1668
4. Leslie, A. G. W., and Walker, J. E. (2000) *Philos. Trans. R. Soc. Lond. B Biol. Sci.* **355,** 465–472
5. Diez, M., Zimmerman, B., Börsch, M., König, M., Schweinberger, E., Steigmiller, S., Reuter, R., Felekyan, S., Kudryavtsev, V., Seidel, C. A. M., and Gräber, P. (2004) *Nat. Struct. Mol. Biol.* **11,** 135–141
6. Itoh, H., Takahashi, A., Adachi, K., Noji, H., Yasuda, R., Yoshida, M., and Kinosita, K. (2004) *Nature* **427,** 465–468
7. Ahmad, Z., and Senior, A. E. (2004) *J. Biol. Chem.* **279,** 31505–31513
8. Menz, R. I., Walker, J. E., and Leslie, A. G. W. (2001) *Cell* **106,** 331–341
9. Braig, K., Menz, R. I., Montgomery, M. G., Leslie, A. G. W., and Walker, J. E. (2000) *Structure* **8,** 567–573
10. Orriss, G. L., Leslie, A. G. W., Braig, K., and Walker, J. E. (1998) *Structure* **6,** 831–837
11. Perez, J. A., Greenfield, A. J., Sutton, R., and Ferguson, S. J. (1986) *FEBS Lett.* **198,** 113–118
12. Weber, J., Lee, R. S. F., Grell, E., Wise, J. G., and Senior, A. E. (1992) J. *Biol. Chem.* **267,** 1712–1718
13. Weber, J., Wilke-Mounts, S., and Senior, A. E. (1994) J. *Biol. Chem.* **269,** 20462–20467
14. Taussky, H. H., and Shorr, E. (1953) J. *Biol. Chem.* **202,** 675–685
15. Senior, A. E., Latchney, L. R., Ferguson, A. M., and Wise, J. G. (1984) *Arch. Biochem. Biophys.* **228,** 49–53
16. Rao, R., Al-Shawi, M. K., and Senior, A. E. (1988) *J. Biol. Chem.* **263,** 5569–5573
17. Weber, J., Wilke-Mounts, S., Lee, R. S. F., Grell, E., and Senior, A. E. (1993) *J. Biol. Chem.* **268,** 20126–20133
18. Klionsky, D. J., Brusilow, W. S. A., and Simoni, R. D. (1984) *J. Bacteriol.* **160,** 1055–1060
19. Ketchum, C. J., Al-Shawi, M. K., and Nakamoto, R. K. (1998) *Biochem. J.* **330,** 707–712
20. Vandeyar, M., Weiner, M., Hutton, C., and Batt, C. (1988) *Gene* (*Amst.*) **65,** 129–133
21. Bradford, M. M. (1976) *Anal. Biochem.* **72,** 248–254
22. Laemmli, U. K. (1970) *Nature* **227,** 680–685
23. Weber, J., and Senior, A. E. (2004) *Methods Enzymol.* **380,** 132–152
24. Löbau, S., Weber, J., Wilke-Mounts, S., and Senior, A. E. (1997) *J. Biol. Chem.* **272,** 3648–3656
25. Weber, J., Hammond, S. T., Wilke-Mounts, S., and Senior, A. E. (1998) *Biochemistry* **37,** 608–614
26. Lunardi, J., Dupuis, A., Garin, J., Issartel, J. P., Michel, L., Chabre, M., and Vignais, P. V. (1988) *Proc. Natl. Acad. Sci. U. S. A.* **85,** 8958–8962
27. Nadanaciva, S., Weber, J., and Senior, A. E. (1999) *J. Biol. Chem.* **274,** 7052–7058
28. Nadanaciva, S., Weber, J., and Senior, A. E. (1999) *Biochemistry* **38,** 7670–7677
29. Nadanaciva, S., Weber, J., and Senior, A. E. (1999) *Biochemistry* **38,** 15493–15499
30. Fisher, A. J., Smith, C. A., Thoden, J. B., Smith, R., Sutoh, K., Holden, H. M., and Rayment, I. (1995) *Biochemistry* **34,** 8960–8972
31. Nadanaciva, S., Weber, J., and Senior, A. E. (2000) *Biochemistry* **39,** 9583–9590
32. Weber, J., and Senior, A. E. (1998) J. *Biol. Chem.* **273,** 33210–33215
33. Dou, C., Grodsky, N. B., Matsui, T., Yoshida, M., and Allison, W. S. (1997) *Biochemistry* **36,** 3719–3727
34. Ferguson, S. J., Lloyd, W. J., Lyons, M. H., and Radda, G. K. (1975) *Eur. J. Biochem.* **54,** 117–126
35. Ferguson, S. J., Lloyd, W. J., and Radda, G. K. (1975) *Eur. J. Biochem.* **54,** 127–133
36. Weber, J., and Senior, A. E. (2000) *Biochim. Biophys. Acta* **1458,** 300–309